Available online at www.sciencedirect.com

ScienceDirect

Energy Procedia 49 (2014) 98 – 108

Energy Procedia

SolarPACES 2013

Optical characterization parameters for line-focusing solar concentrators: measurement procedures and extended simulation results

P. Horta[a,]*, T. Osório[a]

[a]*University of Évora – Renewable Energies BES Chair, Casa Cordovil,Rua Augusto Eduardo Nunes 7, 7000-651 Évora, Portugal*

Abstract

According to the present standards, the optical characterization of line-focusing concentrators follows the quasi-dynamic test method, thus resulting from thermally based experimental measurements. The impact of optical deviations from design conditions on a concentrator optical performance increases with concentration ratio. Adding to this, the geometrical specificities which might be found in line-focus concentrators render important a more thorough optical characterization of such systems.

The present article studies the interest and possibility of using optical simulation data as a complement to the experimental procedures followed in the optical characterization of line-focusing concentrators. Taking into account the isolated and combined impact of the most prominent optical effects in presence, the validation and accuracy of optical models is compared to that of experimental measurements. Additional optical characterization results to be obtained from such models are suggested, complementing the optical parameters previewed in the standards and enabling a higher accuracy in yield calculations.

Selection and peer review by the scientific conference committee of SolarPACES 2013 under responsibility of PSE AG.

Final manuscript published as received without editorial corrections.

Keywords: line-focus concentrators; optical characterization; optical models; ray trace results

* Corresponding author. Tel.: +351-939007572.

E-mail address: phorta@uevora.pt

Selection and peer review by the scientific conference committee of SolarPACES 2013 under responsibility of PSE AG.

Final manuscript published as received without editorial corrections.

doi:10.1016/j.egypro.2014.03.011

1. Introduction

The most recent standards revision on the optical and thermal characterization of solar thermal collectors [1] defines that concentrating collectors shall be tested according to the quasi-dynamic test method (QDT). Presenting a more thorough approach to the optical characterization parameters affecting separately beam and diffuse radiation components (when compared to steady-state method), its use still stands for the determination of optical parameters after thermally based experimental measurements. Originally based on a collector model which had its origin in stationary collectors, whose optical performance depends essentially in transmission-absorption effects, the QDT test method is thus intended to deal with increasingly complex optical systems.

Nomenclature

A	reference area of collector (m^2)	$\dot{Q}$	useful power extracted from collector (W)
A_a	aperture area of collector (m^2)	α	absorptivity
C	concentration factor	ΔT	temperature difference (K)
C_p	specific heat ($Jkg^{-1}K^{-1}$)	$\eta_{0,b}$	peak collector efficiency
CSR	circumsolar ratio	ρ	reflectivity
G_b	direct solar irradiance (Wm^{-2})	σ_{spec}	specular reflection deviation (mrad)
G_d	diffuse solar irradiance (Wm^{-2})	τ	transmissivity
h_t	truncation height (m)	θ	angle of incidence (º)
L	collector length (m)	θ_a	acceptance angle (º)
$\dot{m}$	mass flow (kgs^{-1})	θ_i	angle between the incidence vector and its projection on the transversal plane (º)
n	refraction index		
$\overline{K}$	weighted average IAM values	$\theta_{L,def}$	reference angle in L-direction for determination of IAM. Normally = 0 (º)
K_b	incidence angle modifier for direct radiation		
$K_{\theta d}$	incidence angle modifier for diffuse radiation	$\theta_{T,def}$	reference angle in T-direction for determination of IAM. Normally = 0 (º)
$K_{\theta T}$	transversal incidence angle modifier		
$K_{\theta L}$	longitudinal incidence angle	θ_s	sun disk aperture angle

In view of enhanced accuracy of yield estimation and system dimensioning calculations, the use of increasing concentration factors withstanding operation at increasing temperatures, might render important a due analysis of optical parameters whose determination is not previewed in the standards. The impact of specular reflection deviations, tracking inaccuracies, multi-axial Incidence Angle Modifier (IAM) simplifications or length dependent end loss effects over the system optical performance are examples of such additional parameters, likely to be obtained after optical models of the collector, validated upon experimentally measured optical efficiency values.

The present article addresses the adoption of optical models in the production of extended optical characterization results. After a revision of optical efficiency and IAM measurement procedures, an analysis of the isolated and combined impact of individual optical effects present in line-focusing systems over these parameters is presented. Considering the two most typical line-focus technologies – Parabolic Trough Concentrator (PTC) and Linear Fresnel Reflector (LFR) – such analysis is compared with expected measurement accuracy and experimental validation of optical models is discussed. Finally, the use of extended simulation results addressing multi-axial IAM simplifications or length dependent end loss effects over the system optical performance is discussed, rendering the use of the QDT collector model more accurate and prone to a general technology independent use.

2. Experimental procedures for determination of optical characterization parameters

In spite the present solar collector testing standards [2] omit a specific mention to solar concentration, their most recent revision [1] already establishes a specific framework for the procedures to be adopted in the optical (and thermal characterization) of solar concentrators. When enforced, the new standards might cope with the test of a

broad range of solar collectors, including tracking concentrating collectors for thermal power generation and process heat. Line focus concentrators such as PTC or LFR fall in this category.

According to the new testing framework, if a tracking device is present, it shall be used during testing and the collectors shall be mounted in a way that enables performance testing up to incidence angles of 60 º from all the relevant directions (transversal and longitudinal planes, in biaxial collectors). Also, the collector shall be tested at tilt angles such that the IAM for the collector varies by no more than 2% from its value at normal incidence (referred to as near normal incidence conditions). For a PTC both conditions are met with an EW orientation, testing at high incidence angles in the morning and afternoon and at normal incidence about the solar noon. For a LFR this requires for the collector to be tilted and to be mounted both in the EW and NS directions (depending on the time of the year and latitude). Furthermore, and depending on the testing site latitude, (near) normal incidence conditions might be impossible to achieve for a horizontal mounting.

Concerning the thermal performance test, the quasi-dynamic model and test method is to be used. According to this model and considering only the aspects related with the optical efficiency, (i.e. neglecting thermal losses) follows for the collector power per unit area:

$$\frac{\dot{Q}}{A} = \eta_{0,b} K_b(\theta_L, \theta_T) G_b + \eta_{0,b} K_{\theta d} G_d \tag{1}$$

Whereas diffuse radiation presents a negligible contribution to collector power when dealing with high or very-high concentration ratios (smaller diffuse radiation IAM values), such collector model is of general use for both low and high concentration factor collectors.

The IAM for the beam radiation is defined as the ratio of the peak efficiency at a given angle of incidence and the peak efficiency at a defined reference angle of incidence according to:

$$K_b(\theta_L, \theta_T) = \frac{\eta_{0,b}(\theta_L, \theta_T)}{\eta_{0,b}(\theta_{L,def}, \theta_{T,def})} \tag{2}$$

The standard states that normal incidence (equal to zero) is normally used as the defined angles of incidence $\theta_{L,def}$ and $\theta_{T,def}$, however other values can be chosen if appropriate, e.g. in case the thermal performance cannot be determined under normal incidence. Yet, this approach narrows the usability of the optical parameters obtained to latitudes for which the incidence angles would always be higher than $\theta_{L,def}$ and $\theta_{T,def}$. The composed IAM can be estimated by considering it to be the product of the separate IAM for two perpendicular symmetry planes [3]:

$$K_b(\theta_L, \theta_T) = K_b(\theta_L, 0) K_b(0, \theta_T) \tag{3}$$

One very important parameter for the comparison of different collectors and technologies is the reference area for the calculation of collector irradiation. For such parameter the present standard [2] accepts both the absorber area (it would make no sense for concentrating collectors) or the aperture area. In the present standard revision [1] collector gross area is used as reference area. In the present article aperture area (defined as the horizontal projection, at normal incidence, of the directly irradiated primary reflector and receiver areas) is used as reference area.

3. Analysis of isolated and combined impact of individual optical effects

The optical effects affecting collector efficiency are manifold. Included in the optical efficiency (accounting for their combined effect) are the impacts of materials optical properties, specular reflection deviations in mirrors, manufacturing (design, structure, etc.) deviations or sun shape effects. The IAM (accounting for the angular variation of such optical effects) includes the angular variation of materials properties and optical path length, the angular variation of effective aperture area (for concentrating systems whose primary changes its “shape” with incidence, such as the LFR), tracking inaccuracies and end losses.

In the present section an analysis of the isolated and combined impact of such effects over collector optical characterization parameters – optical efficiency and IAM – is presented, illustrating their range of variation.

While in the past such analysis was only possible after analytical approaches to simple optical designs, the recent and present computational capabilities have rendered possible the extensive use of ray-trace tools in the calculation of the optical performance of generic optical systems. Such is the case of the results presented in this article.

This analysis is based on the most representative line-focus concentrator designs: PTC and LFR concentrators.

Although subject of different articles [4,5], the use of secondary concentrators in PTCs is negligible (inexistent?) in commercially available collectors. On the contrary, few (or none) available LFRs go without some kind of secondary. Such is, off course, the result of the focusing characteristics of both technologies.

For the sake of completion (and comparativeness) a Compound Parabolic Concentrator (CPC) type secondary [6,7] is applied to both basic PTC and LFR geometries. Both secondaries are designed for an acceptance angle defined after the extreme point of the primary under normal incidence conditions (infinitesimal mirror width approach for the LFR). The CPC thus defined is truncated [8] such that all rays coming from a finite source (Pillbox with solar disk angle θ_s = 4.65 mrad) at normal incidence reach the absorber. The simulated geometries are based in 12 m long modules with tubular evacuated receivers (35 mm absorber radius, 62.5 mm outer radius and 5 mm thickness glass tube). Four basic geometries were designed, according to the main features presented on Table 1:

Table 1. Main features of the four geometries.

Case name	Primary reflector	Receiver position	CPC Secondary	Aperture area
PTC / PTC SEC	5.8 m width parabola	1.71 m focal length	none / θ_a = 81.27 º, h_t = 7 mm	69.90 m^2 / 66.74 m^2
LFR / LFR SEC	16 heliostats (0.75 m wide)	7.4 m height	none / θ_a = 48.39 º, h_t = 41 mm	139.58 m^2 / 138.75 m^2

Three main optical effects were analyzed: materials optical properties, source (sun) shape and mirror surface imperfections (specular reflection deviations). Standard material properties were used to describe real collector materials: mirrors: ρ = 0.935 [9]; absorber [10]: α = 0.955; glass: ρ = 0.035; τ = 0.965; n = 1.52 [11].

The beam spread effect due to sun shape or to mirror surface and/or concentrator structure imperfections, e.g., might be regarded as being combined in the beam spread effect of an effective source [12]. Following this approach, simulations were performed considering the combined effect of a specular reflection deviation in mirror surfaces σ_{spec} = 2.5 mrad and a finite source defined by a Buie [13] sun shape profile for CSR = 0.2 (roughly equivalent to an average clear sky condition for line-focus systems, after a Gaussian sun shape approach, σ_{sun} = 4 mrad [12]). Such values might be regarded as a limit to acceptable mirror quality and circumsolar radiation conditions [13] in concentrated solar power (CSP) applications. Four different optical model configurations were defined (see table 2).

Table 2. Definition of optical effects in simulation model configurations.

Simulation configuration	Source	Materials	Surface errors
IDEAL	Point	Ideal	No errors
REALMAT	Point	Real optical properties	No errors
EFFSOURCE	Buie (CSR 20 %)	Ideal	σ_{spec} = 2.5 mrad
FULLEFFECTS	Buie (CSR 20 %)	Real optical properties	σ_{spec} = 2.5 mrad

Ray-trace simulations were performed with an open-source Monte-Carlo ray tracer [14] with a fixed ray density of 3 000 rays/m^2 of aperture area. For high incidence angles, the wave front area decreases resulting on a high ray density and accuracy. In 60 m and 120 m long LFR collectors the number of rays was limited to 500 000 and 1 000 000 rays, respectively. The results obtained for the different geometries and optical model simulation configurations are graphically presented in Figures 1, 2(a) and 2(b). Regarding the results obtained for PTC collector geometries:

- the optical impact of effective source effects is moderate, result related with both the focusing characteristics of this geometry and with the moderate concentration factor used in its design (C = 26.4);

- the adoption of the secondary concentrator stands only for a slight increase in optical efficiency, resulting from a slightly minor impact of effective source effects (the secondary was designed for the same receiver and for a Pillbox source accounting only for the solar disk aperture). This slight impact is also visible in IAM results;
- real material optical properties present the most important impact in optical efficiency results;
- the combined impact of optical effects stands for an optical efficiency reduction of around 20%, when compared to an ideal system and source.

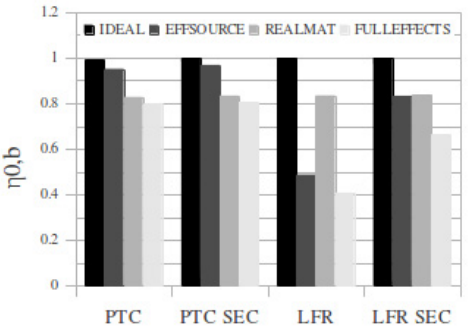

Fig. 1. Optical efficiency results.

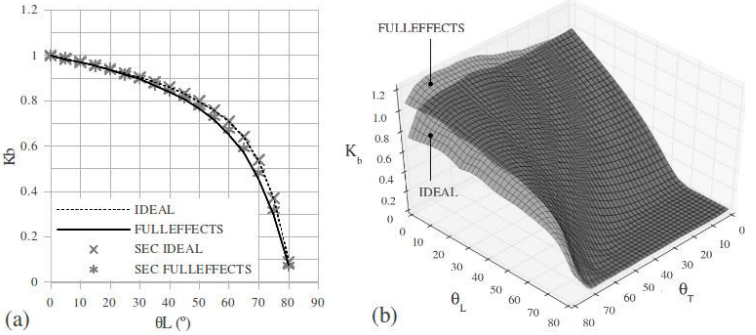

Fig. 2. IAM results for: (a) PTC geometries and (b) **LFR** geometry.

As for the results obtained for LFR collector geometries:

- effective source effects present the most important impact in optical efficiency results, which is especially evident for the **LFR** geometry. This result is related with the focusing characteristics of LFR systems (and explains the "mandatory" use of secondary concentrators in these collectors);
- real material optical properties present also an important impact in optical efficiency results (similar to effective source impacts in the most representative **LFR SEC** geometry);
- the combined impact of optical effects stands for optical efficiency reductions of around 60% and 35% for **LFR** and **LFR SEC** geometries, respectively;
- the most significant difference between PTC and LFR systems is well illustrated in IAM results: PTC geometries present only longitudinal variations; LFR geometries present both longitudinal and transversal variations.

Considering the reference area adopted in IAM calculations, it is important to refer that the transversal variation of IAM in LFR systems is strongly affected by the variation of the effective (irradiated) aperture area of the primary concentrator with transversal incidence (Fig. 3). Considering its importance in the overall system behavior, the impact of tracking inaccuracy over optical performance was also analyzed within ± 1º beam deviations from the system optical axis (Fig. 4). For the LFR primary concentrator results are presented for $\theta_T = 0º$ and $\theta_T = 40º$.

The results presented in Figure 4 illustrate the potential impact of tracking deviations in optical efficiency results, more evident with increased concentration factors with no use of secondary concentrators, as in the **LFR** geometry ($C = 54.6$). The results also illustrate the variation of these impacts with transversal incidence (LFR geometries).

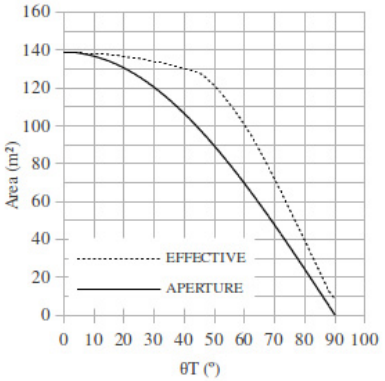

Fig. 3. Variation of effective (irradiated) and aperture areas (wavefront projections) with transversal incidence (**LFR** geometry).

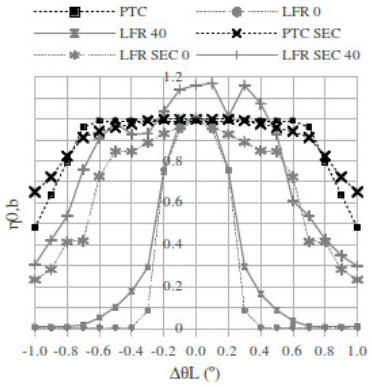

Fig. 4. Impact of tracking deviations in optical efficiency.

4. Experimental validation of optical models

The experimental validation of a solar concentrator optical model derives from a direct comparison of measured and simulated optical efficiency values. Rather than on an exact value, optical efficiency measurements result on best estimation and measurement uncertainty values. Let us consider the limiting situation of an optical efficiency measurement under no thermal loss conditions. From the QDT method, it would follow for the optical efficiency:

$$\eta_{0,b} = \frac{\dot{m} C_p \Delta T}{A\left[K_b(\theta_L, \theta_T) G_b + \eta_{0,b} K_{\theta d} G_d\right]} \tag{4}$$

Further simplifying for a normal incidence condition $K_b(0,0) = 1$ and for a $K_d = 0$ (increasingly reasonable with increasing concentration factors), optical efficiency measurement uncertainty would depend only on flow, fluid temperature difference, aperture area and beam irradiation measurement uncertainties (i.e., these simplifications stand for the minimum uncertainty value). The required accuracy for such parameter measurements is well established in the standards [1,2] and might be summarized according to the following table:

Table 3. Accuracy requirements in the measurement of efficiency test parameters [1,15].

Parameter	Required accuracy
mass flow ($\dot{m}$)	± 1% measured value
fluid temperature difference (ΔT)	± 0.05 K
aperture area (A_a)	± 0.3 %
beam irradiation (G_b)	± 1 %

On the other hand, it is to be expected that different optical simulation tools might present different capabilities. Let us assume five different degrees of capability for such tools, according to the following table:

Table 4. Definition of optical models according to simulation capabilities.

Optical model	Source	Materials	Surface errors
BASIC	Point	Ideal	No errors
MATS	Point	Real optical properties	No errors
SRC+MATS	Pillbox 4.65 mrad	Real optical properties	No errors
SURFS	Pillbox 4.65 mrad	Real optical properties	σ_{spec} = 2.5 mrad
FULL	Buie (*CSR* 5%)	Real optical properties	σ_{spec} = 2.5 mrad

The error sources in optical simulation results are manifold: surface description, beam definition, numerical approximations, wavefront estimation, tracking (and incidence) conditions, etc. At the same time, experimentally measured results depend not only on measurement accuracy but also in a number of optical effects (sun shape, surface errors, tracking deviations, properties), as illustrated in the previous section.

On a first approach, the validation of simulated results could result from a (more or less flexible) adjustment of simulated results to experimental results after a due parametric adjustment of:

- source: sun shape profile reflecting measured irradiation conditions;
- materials: optical properties of absorber, reflector and glazing according to manufacturer specifications;
- surface errors: specular reflection deviations, structural deviations, design deviations after surface characterization techniques for material sample or full reflector surface [16],

so that modeled results would not differ from measured results more than the expected measurement uncertainty.

Considering now the assessment of a threshold on optical model capabilities, let us take as an exact result the one obtained with the FULL simulation tool. A threshold on optical model capabilities could be set assuming (again) as a limit for simulated results variation (from the best result) the uncertainty values obtained for its experimental measurement. The optical efficiency results obtained for the reference collector geometries and for the different optical models described in Table 4 are illustrated in Figure 5. The corresponding measurement uncertainties are represented in the graphic, for each geometry, in the reference FULL optical model result.

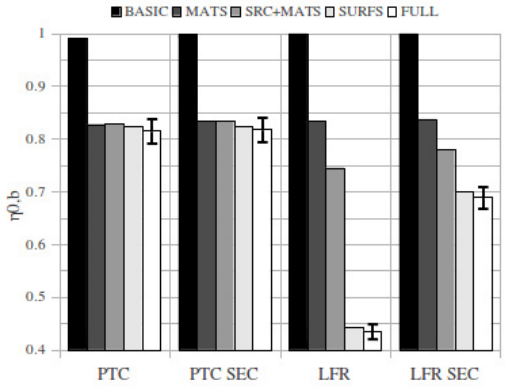

Fig. 5. Optical efficiency results obtained with different simulation capabilities for reference collector geometries (and corresponding experimental measurement uncertainty on reference FULL optical model result).

From the results presented in Figure 5 the following remarks might be made:

- ideal optics, while useful in basic concentrator design, are far from describing the optical behavior of real collectors under real operation conditions and are thus unsuitable for the determination of collector optical characterization parameters;

- the minimum requirements for optical model capabilities depend on the simulated concentrator geometry (not only concentration factor but also effective acceptance angle, as LFR and LFR SEC results illustrate).

A thorough validation would require also an analysis of the IAM results, to be compared with the reference (FULL) optical model results after a point to point or a weighted integration approach.

5. Use of optical models in the production of extended optical characterization results

In brief, the application of the QDT method on the experimental determination of optical characterization parameters of (line-focus) solar concentrators relies on the positioning of the collector at 0 º azimuth reaching normal incidence conditions at solar noon. As a result, optical efficiency values for both beam and diffuse radiation are obtained after a multi-linear regression of thermally based experimental power measurements. Discrete IAM values along the longitudinal and transversal planes are also obtained. Both QDT testing requirements and results pertain some questions when more complex optical systems are in stake: the case of LFR systems.

5.1. Composed IAM

A simple approach to the determination of a composed IAM relying only on the product of the corresponding transversal and longitudinal IAM values was proposed (in the 80's) by McIntire [3] and adopted in the collector testing standards as a suitable method. While providing a good approach when dealing with simple optical systems (say, collectors presenting a "regular" composed IAM), its accuracy falls short when dealing with more complex systems, as already demonstrated, e.g., for stationary CPC [17,18] or LFR concentrators [19].

Better results were obtained, from the same approximation, when using a different incidence angle when calculating the longitudinal IAM: instead of the incidence angle projected on the longitudinal plane (θ_L) the angle between the incidence vector and its projection on the transversal plane (θ_i) [19].

A comparison of composed IAM results obtained directly from optical simulation of from orthogonal based approximations would follow from integration of the obtained IAM surfaces. Yet, considering the impact of the cosine factor in the instantaneous power being affected by the IAM for a given incidence, such integration might be weighted by the cosine of the incidence angle [8,18]. Such weighted average IAM value is thus a measure of the impact of hemispherical optical features of a collector on its overall yield. Weighted average IAM values are presented, in Table 5, for both LFR collector geometries and composed IAM calculation approaches.

Table 5. Weighted average IAM values after optical simulation (FULLEFFECTS) and orthogonal based approximations.

Collector geometry	$\overline{K}_{sim}$	$\overline{K}$ McIntire	$\Delta\overline{K}$	$\overline{K}_{\theta i}$	$\Delta\overline{K}$
LFR SEC	0.678	0.524	-22.67%	0.666	-1.65%
LFR	0.620	0.475	-23.37%	0.596	-3.81%

Taking as most accurate the result obtained with a (experimentally validated) optical model, it is evident from the presented results that the McIntire approach does not cope with the optical specificities of more complex optical systems. Yet, the modification of this approach with θ_i stands for a very significant improvement on the final results obtained for a orthogonal based composed IAM calculation, as illustrated in Figure 6, yet at the cost of calculating one additional decomposition of the incidence angle.

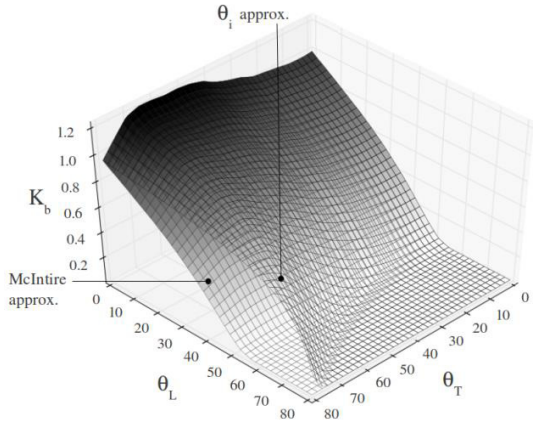

Fig. 6. Composed IAM approximations obtained after McIntire and θ_i approaches for LFR SEC FULLEFFECTS geometry.

5.2. End loss effects

Application of the standard efficiency measurement procedures implies (in the absence of clearly defined *in-situ* measurement procedures) the installation of the solar collector in a dedicated testing bench. When dealing with line-focus concentrators, it is likely that single collector modules (limited in length) are to be transported and tested.

Table 6. Weighted average IAM values after optical simulation (IDEAL) and orthogonal based approximations.

Collector geometry	$\overline{K}_{sim}$	$\overline{K}$ McIntire	$\Delta\overline{K}$	$\overline{K}_{\theta i}$	$\Delta\overline{K}$
LFR SEC 12 m	0.632	0.485	-23.33%	0.621	-1.87%
LFR SEC 60 m	1.061	0.995	-6.19%	1.055	-0.60%
LFR SEC 120 m	1.078	1.048	-2.47%	1.074	-0.37%

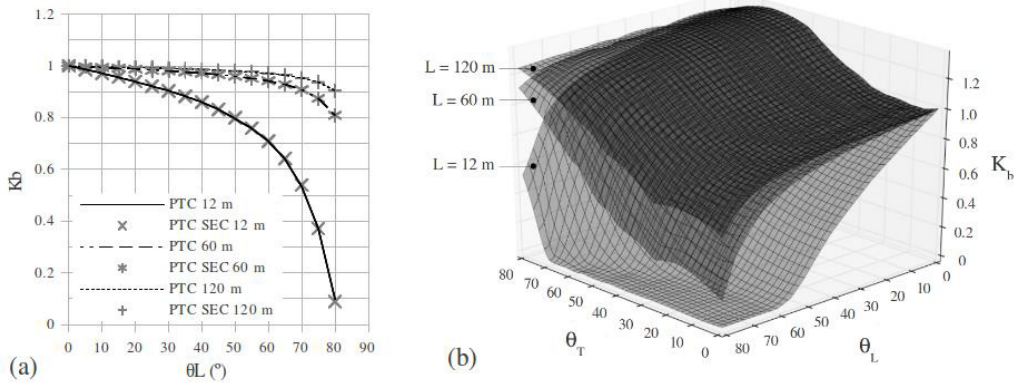

Fig. 7. Composed IAM for a 12 m, 60 m and 120 m long: (a) PTC IDEAL (b) LFR SEC IDEAL.

Experimentally measured longitudinal IAM results are, thus, strongly affected by end loss effects. While suitable analytical expressions are available for a longitudinal length based IAM correction [3,12], such approach is not viable when dealing with composed IAM values affected either on the longitudinal and transversal directions. Such is the case of the LFR, as illustrated in Figure 7(b) for 12 m, 60 m and 100 m long concentrators, for whose weighted average IAM values are presented in table 6.

These results illustrate the impact of collector length in both the composed IAM (see the weighted averaged results, standing for increasingly "filled" composed IAM surfaces) and on orthogonal based composed IAM

approximation results. In the absence of a general analytical expression (as for PTCs) enabling a due length based correction of the IAM, on the form of equation (5), longitudinal (and composed) IAM results for different collector lengths might be produced after simulation results with a validated optical model.

$$K_b(\theta) = K_{b,1MOD}(\theta) f(L) \tag{5}$$

5.3. Normal incidence conditions

Considering the QDT method procedures, (near) normal incidence conditions at collector aperture are required around solar noon. Such requirement is easily met for collectors not presenting transversal incidence effects (such as the PTC): use of an azimuthal tracking platform, enabling a permanent transversal normal incidence while controlling the transversal incidence with the collector one-axis tracking system.

For collectors where transversal incidence effects are present (such as LFR concentrators), (near) normal incidence conditions can be met only in a very limited (or even at none) period of the year, at say over tropical latitudes. An increased period with near normal conditions would require, for such collectors, a platform with both azimuthal tracking and variable tilt angle (besides the use of the collector own one-axis tracking system).

An attempt to alleviate such requirements was introduced in the last standards revision [1]. Taking into account both the unavailability of a dual-axis tracking platform accommodating real size LFR modules and/or the technical difficulties arising from tilting real size LFR modules, an optional "off-normal" based IAM is defined.

Whereas such approach enables the calculation of IAM without a normal incidence based reference optical efficiency, it does not produce, on its own, real information regarding the optical behavior of the collector when subjected to such normal incidence conditions (for the sake of a geographical independent parameter usability).

Again, such results might be produced after simulation with an experimentally validated optical model.

6. Conclusions

The most recent revision of the standards on the optical and thermal characterization of solar thermal collectors establishes a framework of procedures to be adopted in the testing of (line-focus) solar concentrators. The optical characterization of the collector relies in optical efficiency and discrete IAM values (on both transversal and longitudinal planes). As already observed in LFR concentrators, such parameters might fall short when accurately describing the optical performance of complex systems. On the other hand, the application of testing procedures (under normal incidence conditions) might be of difficult application in over tropical latitudes, namely for LFR concentrators.

The present article addresses the interest of using optical simulation data as a complement to the experimental procedures followed in the optical characterization of line-focusing concentrators. Such possibility must rely in a due validation, by comparison with standard testing measurements, of an optical model whose accuracy might be enhanced after additional information on materials properties, optical errors or sun shape.

Experimental measurement uncertainties already defined in the testing standard, establish a threshold to optical model capabilities. This criterion enables the classification of different optical simulation tools in terms of their ability to produce acceptable optical characterization results.

The use of a validated optical model, apart from other custom detailed analyses, enables the production of additional and complementary optical characterization results for composed IAM or length based end loss effects correction. Their use might also render viable the production of normal incidence results after off-normal incidence testing measurements.

Not previewed in the recent standards revision, the adoption of simulation models in future revisions presents then open questions on simulation tool classification, additional information on collector materials, circumsolar conditions or collector testing output results.

Acknowledgements

The authors wish to acknowledge the Portuguese funding institution – Fundação para a Ciência e a Tecnologia (FCT) – for supporting their research.

References

[1] ISO/FDIS 9806:2013, Solar energy - Solar thermal collectors - Test methods. Under voting.
[2] EN 12975-2 Thermal solar systems and components – Solar collectors – Part 2: Test methods. European Committee for Standardization; 2006.
[3] McIntire W. Factored approximations for biaxial incident angle modifiers. Solar Energy 1982;29-4.
[4] Collares-Pereira M, et al. High concentration two-stage optics for parabolic trough solar collectors with tubular absorber and large rim angle. Solar Energy 1991;47-6.
[5] Feuermann D, Gordon J, Ries H. High-Flux solar concentration with Imaging designs. Solar Energy 1999;65-2.
[6] Winston R, et al. Nonimaging Optics. Elsevier Academic Press; 2005.
[7] Chaves J. Introduction to Nonimaging Optics. CRC Press; 2008.
[8] Carvalho MJ, et al. Truncation of CPC Solar Collectors and its effect on energy calculations. Solar Energy 1985;35-5.
[9] National Renewable Energy Laboratory, U.S. DoE, http://www.nrel.gov/csp/troughnet/solar_field.html, [Accessed April 2013]
[10] SCHOTT Solar CSP GmbH, SCHOTT PTR®70 Receiver, http://www.schott.com/csp/english/download/ptr70_receiver_brochure.pdf [Accessed April 2013]
[11] SCHOTT AG, SCHOTT Technical Glasses - Physical and technical properties, 2010 http://www.schott.com/tubing/english/download/schott-tubing_brochure_technical-glasses_english.pdf [Accessed May 2013]
[12] Rabl A. Active Solar Collectors and Their Applications. Oxford University Press; 1985.
[13] Buie D, Monger AG, Dey CJ. Sunshape distributions for terrestrial solar simulations. Solar Energy 2003;74-2.
[14] Tonatiuh release 2.0.1, http://code.google.com/p/tonatiuh/
[15] http://www.estif.org/solarkeymarknew/projects/solar-keymark-ii-project
[16] Bernhard R, et al. Linear Fresnel Collector Demonstration on the PSA Part I – Design, Construction and Quality Control. In: Proceedings of the 14th SolarPACES International Symposium. Las Vegas, USA; 2008.
[17] Rönnelid M, Perers B, Karlsson B. On the factorization of incidence angle modifiers for CPC collectors. Solar Energy 1997;59-4.
[18] Carvalho MJ, et al. Incidence Angle Modifiers: a general approach for energy calculations. In: Proceedings of ISES Solar World Congress. Beijing; 2007.
[19] Bernhard R, et al. Linear Fresnel Collector Demonstration on the PSA Part II – Commissioning and first Performance Tests. In: Proceedings of the 14th SolarPACES International Symposium. Las Vegas, USA; 2008.